TOWARDS NUMERICAL SIMULATION OF YARN INSERTION ON AIR-JET WEAVING LOOMS

Delcour Lucas[1], Van Langenhove Lieva[2], Degroote Joris[1,3]
[1] Ghent University, Department of Electrical Energy, Metals, Mechanical Constructions & Systems, Belgium, 9000 Ghent
[2] Ghent University, Department of Materials, Textiles and Chemical Engineering, Belgium, 9000 Ghent
[3] Flanders Make, Belgium

Abstract

In this research a structural solver and flow solver are coupled to simulate the motion of a nylon yarn as it is launched into the atmosphere by a main nozzle of an air-jet weaving loom. The high-speed air flow, large displacements of the yarn, 3D-nature of the problem and the contact between yarn and nozzle wall pose substantial challenges to both solvers. Furthermore, the large displacements necessitate a two-way coupling which drastically increases the computational time required.

In fluid-structure interaction simulations, the flexible structure is often modelled using continuum elements. However, in this work, the use of beam theory to model the yarn is investigated. Switching to beam theory allows reducing the computational time required for the structural solver, but requires adaptations to the fluid-structure interaction code so that forces are projected onto the centreline and centreline displacements are converted into 3D displacements of the surface nodes.

To validate the use of beam elements, a structural simulation is performed in which a section of the yarn is mechanically pulled through the main nozzle. Afterwards the correct functioning of the beam elements is tested by performing a fluid-structure interaction simulation on a 3D, cantilevered beam in cross-flow. Finally, a simulation is performed in which a nylon yarn (diameter 0.72 mm) is unwound by the main nozzle air flow (5 bar gauge) and launched into the atmosphere. The gain in computational time by switching to beam elements is evaluated.

Introduction

Air-jet weaving looms can produce fabric at a very high rate, making them well suited for mass production of fabrics. In that regard, failed insertions need to be avoided as much as possible. A failed insertion can occur due to for example the yarn being blown out of the reed channel or yarn breakage. Currently, failed insertions are avoided by carefully tuning the position of the

lex geometry of such a machine makes it difficult to assess the influence of parameter changes on the air flow and the effect this has on the yarn transport. Therefore, numerical modelling of the insertion process could provide additional insight and lead to a more reliable insertion.

The first models for yarn insertion usually relied on approximate analytical and empirical models for the air flow, yarn tension and air-yarn friction. Uno [1] did so to calculate the yarn velocity of a yarn launched by a main nozzle, Salama et al. [2] to investigate the use of several configurations of the insertion tube and Adanur and Mohamed [3] to compare the yarn tension for several yarn storage devices.

Over the years the productivity of the weaving looms has increased substantially but the machines themselves have also become more complex. To further improve the machines the models have to deal with additional complexities and/or yield more accurate results. Consequently, more and more numerical research is being performed. For air-jet weaving looms these numerical methods are typically finite element models (FEM) for the yarn and the machine components and computational fluid dynamics (CFD) for the air flow. When trying to model/simulate the behaviour of a yarn, the interaction between the yarn and the surrounding air has to be captured, which is done in so-called fluid-structure interaction (FSI) simulations.

CFD simulations have, for example, been used by Oh et al. [4], Kim et al. [5], Chen et al. [6] and Jin et al. [7] to study the air flow inside the main nozzle and/or improve the main nozzle design. CFD studies of the relay nozzle have been conducted by e.g. Adamek et al. [8] and Schröter et al. [9]. Adamek et al. also investigated the interaction of the main nozzle flow with the reed and the influence of the reed dent shape thereon.

In air-jet weaving looms the yarn moves by interaction with the air flow. The yarn itself is a very long and slender structure and undergoes large scale motions during insertion. The modelling of its motion is not straightforward even using numerical tools. In some cases the effect of the moving structure (in this case the yarn) on the flow field can be neglected. Simulations in which the flow exerts forces on the structure but not vice-versa are referred to as one-way coupled simulations. Tang and Advani [10] performed such simulations on a single fiber and on 2 interacting fibers in a simple shear flow. This was one of the first times that a combined model (computational structural mechanics and CFD) was applied to high aspect ratio fibers. Other, more recent, one-way coupled simulations were performed by: De Meulemeester, Githaiga et al. [11] (simulation of the yarn tension during braking), De Meulemeester et al. [12] (simulation of the yarn unwinding from a drum by a main nozzle) and Battochio et al. [13] (simulation of a long fiber in a uniform turbulent flow).

In some cases, however, it is important to also capture the influence of the moving structure on the flow. These simulations are typically referred to as two-way coupled. In the main nozzle of an air-jet weaving loom the yarn occupies a relatively large section of the flow area and its motion can substantially affect the flow, which in turn can alter the yarn behavior upon exiting the nozzle. Two-way coupling, however, drastically increases the computational cost. Consequently, most two-way coupled simulations have been performed for a 2D or 2D-axisymmetric flow field, as was done by Zeng et al. [14] and Osman, Malengier et al. [15]. A 3D simulation of the yarn motion inside the main nozzle of an air-jet loom with the yarn clamped at the inlet was performed by Osman et al. [16].

In this research a 3D two-way coupled simulation of a yarn launched by a main nozzle is performed. The computational cost is limited by modelling the yarn using beam elements, by using an explicit coupling and by limiting the extent of the flow domain. The validity of the beam elements model is first investigated and the explicit coupling is compared to an implicit coupling to assess the influence.

Methodology

As was mentioned in the introduction a two-way coupled FSI-simulation of a yarn launched by the main nozzle will be performed in this research. This implies that both a flow and a structural model have to be created. Firstly, the configuration of the flow solver will be discussed, followed by a description of the structural model and the coupling algorithm. The models used for test cases will shortly be described in the corresponding section.

Flow model - Yarn launch

The goal of the flow model is to calculate the air flow generated by the main nozzle and extract from this flow field the forces acting on the yarn. An illustration of the flow model is displayed in Figure 1. The flow domain extends up to 20 cm behind the main nozzle exit.

To capture the influence of the yarn (motion) on the flow and forces, it has to be included in the flow solver. In the current research this is done by using a Chimera technique. With a Chimera technique grids are superimposed and the solution is obtained by interpolating data between overlapping sections of the grids and using that interpolated data as a boundary condition. For the case at hand a single background grid and a single component grid is used. The background grid contains the entire flow domain and remains stationary. The component grid is a cylindrical grid (diameter = 2 mm) around the yarn (diameter = 0.72 mm) extending slightly beyond the ends of the yarn. The outer surface of the component grid constitutes the Chimera interface. This boundary has to be closed and surround the entire component mesh. The interpolation does not necessarily occur at this interface. The yarn surface is considered as a no-slip wall and its displacement is obtained from the coupling code based on data obtained from the structural solver. The component mesh will follow the motion of the yarn as close as possible to avoid mesh degradation, to this end the component mesh is treated as a linear elastic solid with a poisson coefficient of 0.

The background mesh consists of approximately 500 000 hexahedral cells and the component mesh contains about 3.8 million hexahedral cells. The large number of cells in the component mesh is orginates from the fact that almost the entire length of yarn has to pass through the shock region inside the main nozzle, where a fine mesh resolution is required. During the calculation, however, a lot of the cells in the component mesh are located outside of the background mesh and are, thus, not actively included in the simulation. These cells will be activated once they enter the domain due to the unwinding of the yarn and will be deactivated again once they exit the flow domain on the downstream side.

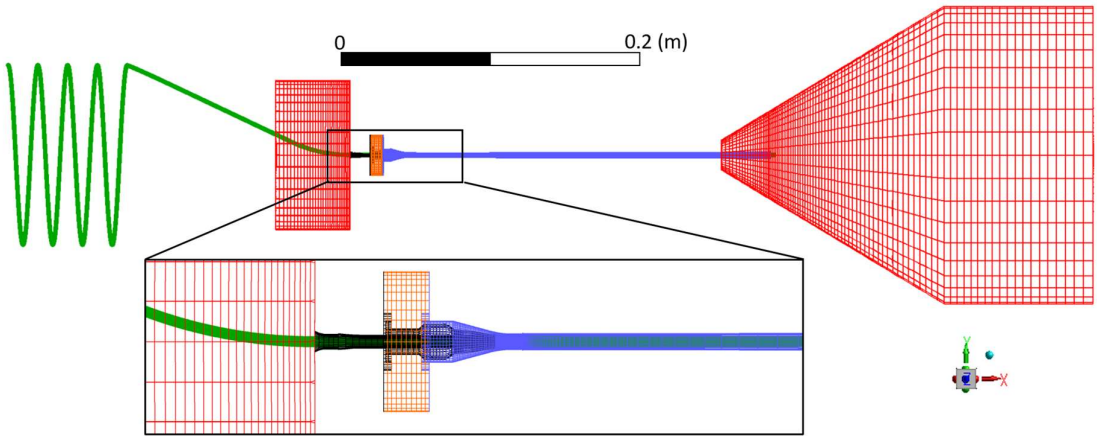

Figure 1: Flow model used for the simulation of the yarn launch. Orange = air inlet (total pressure imposed); Blue = tube wall (no-slip); Red = pressure outlet (static pressure imposed); Black = rocket wall (no-slip); Green = Chimera interface.

Transient calculations were performed with a time step size of 5e-06 s. As a turbulence model the k-ω SST model was used. The flow was initialized with a velocity of 0 m/s in the entire domain and a pressure of 100 000 Pa. At time 0 a total pressure of approximately 5 bar is imposed at the inlet. The flow simulations were performed with Ansys Fluent 18.2.

Structural model - Yarn launch

The structural model is shown in Figure 2. It consists of 2 parts: the yarn and a simplified representation of the main nozzle. As was mentioned previously, the yarn is modelled using beam elements; the validaty of this approach is discussed later on. The yarn has a total length of 1.98 m and is meshed with 990 beam elements. The material is nylon with a density of 1140 kg/m³, a Young's modulus of 2.5 GPa and a Poisson coefficient of 0.39. The yarn is clamped at its leftmost end and free on the other end.

A contact boundary condition is implemented between the yarn centerline and the analytical rigid body. The analytical rigid body is prepended with a funnel to smoothen out the contact as the yarn enters the nozzle. The radius of the body (R_{body}) is given by:

$$R_{body} = 0.85 \cdot (radius\ of\ the\ main\ nozzle) - (radius\ of\ the\ yarn)$$

The factor of 0.85 was implemented so that in the flow solver there is always some space in between the nozzle wall and the yarn wall as required by the Chimera technique. By refining the mesh in the flow solver it would be possible to reduce this spacing at the cost of additional computational time. Zero spacing between the nozzle wall and the yarn wall in the flow solver can, however, not be achieved with the current methodology. Furthermore, the radius of the yarn has to be subtracted as the contact is acting on the centerline instead of the outer yarn surface. The structural simulations are performed in Abaqus 6.14.

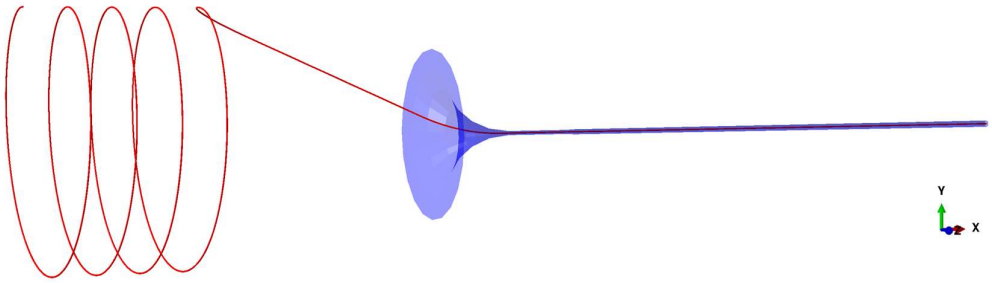

Figure 2: Structural model used for the simulation of the yarn launch. Blue = contact surface (analytical rigid body); Red = Centerline of the yarn.

Coupling

To couple both solvers an in-house code name “Tango” is used, which employs a partitioned approach. The coupling can be either implicit or explicit. With an explicit coupling, forces are extracted from the flow solver and these forces are then passed to the structural solver which subsequently calculates the new position of the structure at the end of the time step and passes this position back to the flow solver to use in its next time step. With an implicit coupling the structural and flow solver are executed multiple times within a single time step. These coupling iterations are stopped once the calculated displacement and/or force of iteration *k* is sufficiently close to those calculated in iteration *k-1*. The main calculation in this research is performed with an explicit coupling as this yields a faster calculation. The first part of the calculation is also compared to an implicit coupling.

Normally, when a continuum mesh is used for the structure, the structural solver calculates the displacement of points on the outer surface, these displacements are then interpolated to the nodes on the surface mesh of the flow solver. However, with beam elements, the displacements of the centerline are calculated. The coupling code then has to translate this to nodal displacements for the flow solver. Additionally, forces in the flow solver are calculated as acting on the surface of the structure. When using beam elements these forces have to be added and assigned to the correct part of the centerline. In this research these complications have been dealt with by using a structured grid on the yarn surface and grouping the nodes and faces on the yarn surface into rings. Each ring has its own centreline coordinate and interpolation/exchange of the data between the solvers is based on the centreline coordinate and ring thickness. When a new centreline position is obtained from the structural solver, the geometrical transformation between the current and the previous state is calculated for each ring and subsequently applied.

Beam elements

Structural test

To validate the use of beam elements for the yarn structure a structural simulation is performed with both continuum elements and beam elements in which a fixed axial force (0.8 N) is imposed at the yarn tip for 0.02 s. The position of the yarn after 0.2 s is shown in Figure 3, the tip position as a function of time is shown in Figure 4. These plots show that there is practically no difference between both simulations.

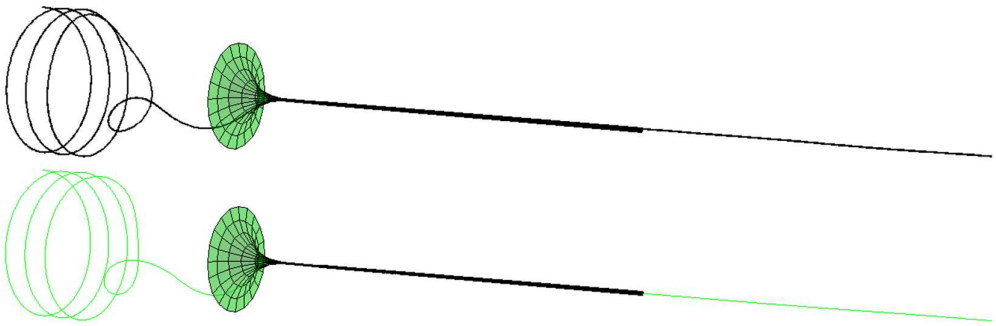

Figure 3: End position of the structural test for beam elements. Top = Continuum elements; Bottom = Beam elements.

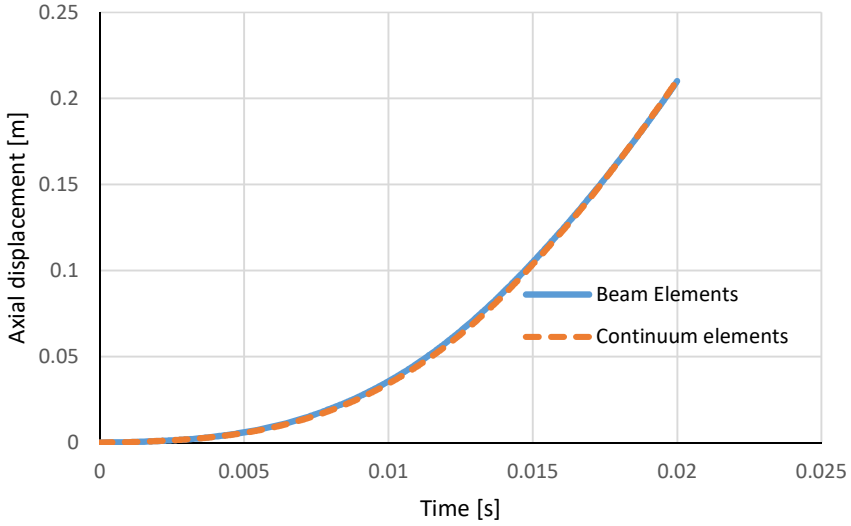

Figure 4: Axial tip displacement during structural test for beam elements and continuum elements.

FSI test

To validate the correctness of the adaptations to the coupling code and the manner in which the forces and displacements were interpolated and applied, an FSI simulation was performed for a flexible plate subjected to a cross flow. The simulation is performed one time using continuum elements and one time using beam elements to model the plate.

The structural characteristics of the plate are given in Table 1. The plate is clamped at the lower edge. When this plate is subjected to a cross-flow it will take on a steady-state displacement. Therefore, the FSI simulation is also performed in steady state. Additionally, to better test the implementation, the setup was three-dimensional. A contour plot of the velocity magnitude in the central plane at the end of the simulation is shown in Figure 5 along with a visualization of the mesh near the tip of the plate. The flow domain is a box with dimensions 0.21 m x 0.17 m x 0.16 m. Water enters the domain from the left side with a velocity of 0.1606 m/s. On the right side of the domain a static pressure of 0 Pa is imposed. The fluid is considered incompressible. The remaining exterior boundary faces of the domain are set as a symmetry boundary condition so that the flow is parallel to these surfaces. With the continuum elements model a horizontal tip displacement of 2.53 cm and a vertical tip displacement of -0.79 cm was calculated. The model with beam elements resulted in a horizontal tip displacement of 2.58 cm and a vertical tip displacement of -0.75 cm. The difference in displacement is partly caused by

the fact that in the current beam elements model, the force on the top surface of the plate is neglected. The small difference between both simulations indicates that the implementation of the model is adequate.

Table 1: Structural parameters of the cantilevered plate.

Height (L)	0.05 m
Width (b)	0.01 m
Thickness (t)	0.002 m
Youngs modulus	491226 Pa
Poisson coefficient	0.4

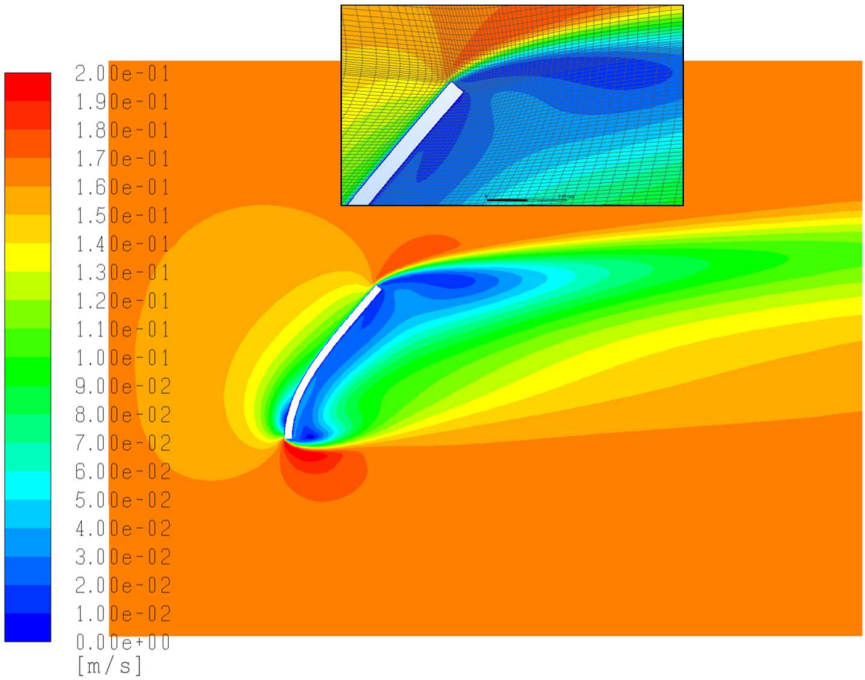

Figure 5: Contour of velocity magnitude at the end of the simulation.

Results

In this section, the FSI simulations of the yarn launched from the main nozzle are presented. The simulation was continued until the yarn (which is clamped at its leftmost end) was completely unwound by the main nozzle. As mentioned in the methodology section the flow domain only extends up to 20 cm beyond the nozzle exit. As the yarn has a total length of approximately 2 m, this implies that the yarn will partly leave the domain again. Cells from the component mesh that exit the flow domain (the background mesh) are excluded from the calculation and retain the values they had prior to their exit. Based on these values and the yarn motion, which is imposed, the forces are updated. The flow variables in those cells are, however, not completely correct as they are not calculated. However, the flow velocity and pressure towards the end of the domain are close to 0 m/s and atmospheric pressure so the impact of this error on the unwinding of the yarn will be rather limited as the axial force will largely be correct. Nevertheless, the free end of the yarn is quite sensitive to the flow and consequently its oscillatory behavior will not be representative after some time. This can however be fixed by extending the background mesh further downstream at the cost of extra computational time.

Figure 6 shows a comparison between the yarn velocity at the nozzle exit for the implicit and the explicit calculation. Apart from some fluctuations, both calculations predict the same behavior with the yarn speed levelling off at about 19.5 m/s.

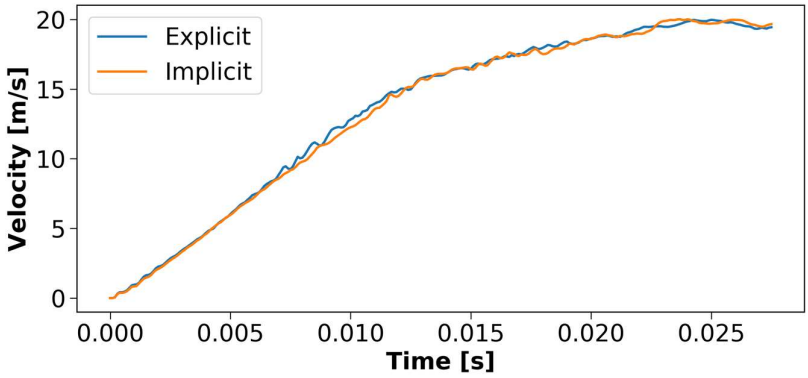

Figure 6: Velocity of the yarn at the nozzle exit.

The vertical displacement of the yarn at a location 7 mm beyond the nozzle exit is displayed in Figure 7. Quite some difference can be observed between the calculations in terms of vertical displacement. In FSI, a small difference at a certain time can cause large differences further along the line. Overall, the amplitude of the oscillations predicted by both methods is similar: the implicit and explicit simulation yield a maximal peak-to-peak amplitude of 2.95 mm and 2.63 mm respectively. The explicit method shows some higher frequency behavior than the implicit one.

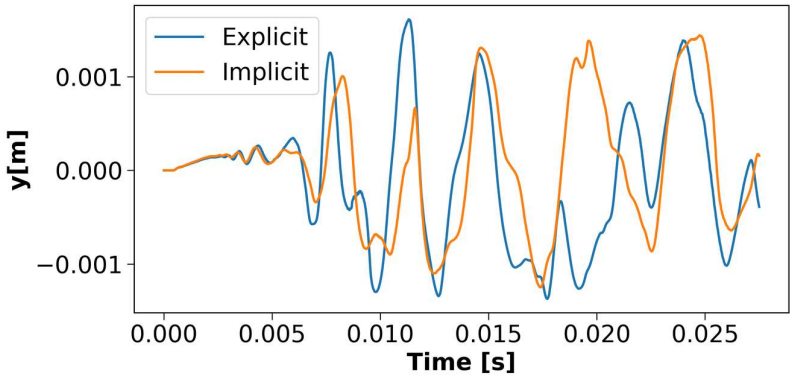

Figure 7: Vertical displacement of the yarn at a distance of 7 mm from the nozzle exit.

The explicit method employs a staggered approach while the implicit method corrects the displacement in each time step based on coupling iterations. If one is interested in the exact oscillation behavior of the yarn an implicit method should be opted for (unless the time step is chosen even smaller). Nevertheless, an explicit method could suffice to generate an idea about the amplitude of the oscillation. As the explicit method allows for a faster computation and since the main goal of the current research was to analyse the feasibility of such simulations, the explicit simulation was continued in time until the yarn was fully unwound.

Figure 8 shows the position of the yarn at several time instants. Figure 9 displays the velocity magnitude of the yarn at the nozzle exit and Figure 10 depicts the vertical yarn oscillation 7 mm downstream of the nozzle exit.

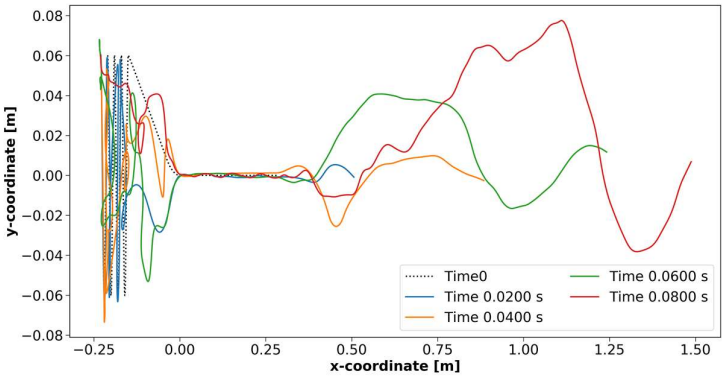

Figure 8: Position of the yarn in the x-y plane at several time instants as obtained from the explicit simulation.

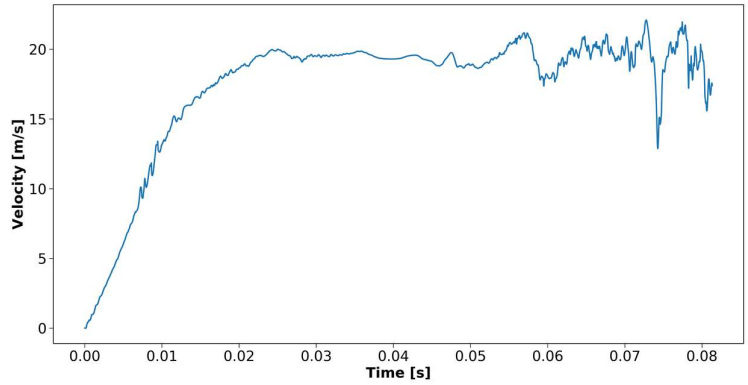

Figure 9: Velocity magnitude of the yarn at the nozzle exit as obtained from the explicit simulation.

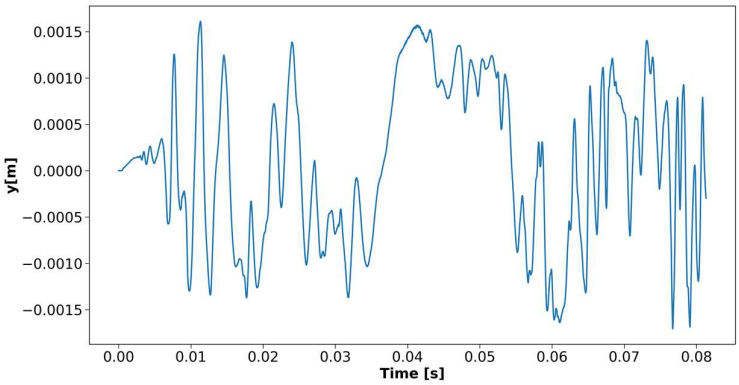

Figure 10: Vertical displacement of the yarn at a location 7 mm downstream of the nozzle exit as obtained from the explicit simulation.

The total simulation time amounted to about 105 full days on 20 cores of the type Intel Xeon E5-2680v3 2.5GHz. Approximately 74% of the time was spent in the flow solver and 3% in the structural solver. As a lot of time is spent solving the flow, a substantial reduction in simulation time could be obtained by executing the flow solver on more cores. The gain in computational time by switching to beam elements was approximately 10%.

Conclusion

In this research a 3D FSI simulation of a yarn launched by the main nozzle of an air-jet weaving loom was performed. To save on computational time the yarn was modelled using beam elements, which required adaptations to the coupling software. The validity of using beam elements for the structure and the implementation into the coupling software was tested. The final simulation was performed using an explicit coupling method to further reduce the computational cost. In the end it was possible to simulate a complete unwinding of the yarn. The accuracy of the simulations could be improved by extending the flow domain further downstream and using an implicit coupling algorithm.

Acknowledgements

The computational resources (Stevin Supercomputer Infrastructure) and services used in this work were provided by the VSC (Flemish Supercomputer Center), funded by Ghent University, FWO and the Flemish Government department EWI.

Literature

[1] Uno M., A study on air-jet loom with substreams added, Part 1: Deriving the equation of motion for weft; Journal of the Textile Machinery Society of Japan vol. 57, pp. 48-56, (1972).

[2] Salama M., Adanur M., and Mohamed M. H., Mechanics of a single nozzle air-jet filling insertion system, Part III: Yarn insertion through tubes; Textile Research Journal vol. 57, pp. 44-54, (1987).

[3] Adanur S., and Mohamed M. H., Analysis of yarn tension in air-jet filling insertion; Textile Research Journal vol. 61, pp. 259-266, (1991).

[4] Oh T. H., Kim S. D., and Song D. J., A numerical analysis of transonic/supersonic flows in the axisymmetric main nozzle of an air-jet loom; Textile Research Journal vol. 71, no. 9, pp. 783-790, (2001).

[5] Kim H.-D. Lim C.-M. Lee H.-J. and Chun D.-H. A study of the gas flow through air jet loom; Journal of Thermal Science vol. 16, no. 2, pp. 159-163, (2007).

[6] Chen L., Feng Z.-h. Dong T.-z. Wang W.-h. and Liu S., Numerical simulation of the internal field of a new main nozzle in an air-jet loom based on Fluent; Textile Research Journal vol. 85, no. 15, pp. 1590-1601, (2015).

[7] Jin Y., Cui J., Zhu L., Lin P., and Hu X., An investigation of some parameter effects on the internal flow characteristics in the main nozzle; Textile Research Journal vol. 87, no. 1, pp. 91-101, (2017).

[8] Adamek K., Karel P., Kolar J., Jirku S., Kopecky V., and Pelant J., Relay nozzles and weaving reed; International Journal of Mechanical Engineering and Applications vol. 3, no. 1, pp. 13-21, (2015).

[9] Schröter A., Schwarzfischer F., Grassi C., Gloy Y.-S. Corves B., and Gries T., Analysis of the Weft Insertion Process and Development of a Relay Nozzle Concept for Air-Jet Weaving; Tekstilec vol. 59, no. 2, pp. 182-185, (2016).

[10] Tang W., and Advani S., Dynamic simulations of long flexible fibers in shear flow; CMES vol. 8, pp. 165-176, (2005).

[11] De Meulemeester S., Githaiga S., and Van Langenhove L., Simulation of the dynamic yarn behavior on airjet looms; Textile Research Journal vol. 75, pp. 724-730, (2005).

[12] De Meulemeester S., Van Langenhove and Van Langenhove L., Three-dimensional simulation of the dynamic yarn behavior on air-jet looms; Textile Research Journal vol. 79, pp. 1706-1714, (2009).

[13] Battochio F., Sutcliffe M. P. F., and Teschner F., Dynamic simulation of long polymeric fibres immersed in a turbulent air flow; The 2nd Joint International Conference on Multibody System Dynamics, Stuttgart, Germany (2012).

[14] Zeng Y. C., Yang J. P., and Yu C. W., Mixed Euler-Lagrange approach to modeling fiber motion in high speed air flow; Applied Mathematical Modelling vol. 29, pp. 253-261, (2005).

[15] Osman A., Malengier A., De Meulemeester S., Peeters J., Vierendeels J., and Degroote J., Simulation of air flow-yarn interaction inside the main nozzle of an air jet loom; Textile Research Journal vol. 88, no. 10, pp. 1173-1183, (2017).

[16] Osman A., Delcour L., Hertens I., Vierendeels J., and Degroote J., Toward three-dimensional modeling of the interaction between the air flow and a clamped-free yarn inside the main nozzle of an air jet loom; Textile Research Journal vol. 89, no. 6, pp. 914-925, (2019).